Assessment of factors influencing groundwater-level change using groundwater flow simulation, considering vertical infiltration from rice-planted and crop-rotated paddy fields in Japan

Yumi Iwasaki*, Kimihito Nakamura, Haruhiko Horino, Shigeto Kawashima

Y. Iwasaki, K. Nakamura, S. Kawashima

Graduate School of Agriculture, Kyoto University

Kitashirakawa Oiwake-cho, Sakyo-ku, Kyoto 606-8502, Japan

e-mail: iwasaki.yumi.26m@st.kyoto-u.ac.jp

H. Horino

Graduate School of Life and Environmental Sciences, Osaka Prefecture University

1-1 Gakuen-cho, Naka-ku, Sakai, Osaka 599-8531, Japan

*Corresponding author:iwasaki.yumi.26m@st.kyoto-u.ac.jp

Tel: +81-75-753-6175

Fax: +81-75-753-6476

Abstract

Assessing factors, such as land use and pumping strategy, that influence groundwater levels is essential to adequately manage groundwater resources. A transient numerical model for groundwater flow with infiltration was developed for the Tedori River alluvial fan (140 km^2), Japan. The main water input into the groundwater body in this area is irrigation water, which is significantly influenced by land use, namely paddy and upland fields. The proposed model consists of two models, a one-dimensional (1-D) unsaturated-zone water flow model (HYDRUS-1D) for estimating groundwater recharge and a 3-D groundwater flow model (MODFLOW). Numerical simulation of groundwater flow from November 1975 to 2009 was performed to validate the model. Simulation revealed seasonal groundwater level fluctuations, affected by paddy irrigation management. However, computational accuracy was limited by the spatiotemporal data resolution of the groundwater use. Both annual groundwater levels and recharge during the irrigation periods from 1975 to 2009 showed long-term decreasing trends. With the decline in rice-planted- paddy field area, groundwater recharge cumulatively decreased to 61 % of the peak in 1977. A paddy–upland crop rotation system could decrease groundwater recharge to 2– 27 % relative to no crop rotation system.

Keywords: groundwater recharge/water budget, paddy field, HYDRUS-1D, MODFLOW, Japan

1. Introduction

The Tedori River alluvial fan in Ishikawa Prefecture, Japan, has abundant groundwater storage capacity. Groundwater in this area is an indispensable water source for drinking and industrial uses and thus supports a variety of anthropogenic activities owing to its stable quantity and quality. Paddy fields covered 45% of this area in 2009; accordingly, water infiltration from the paddy fields during irrigation periods contributes significantly to groundwater recharge (Mitsuno et al. 1982; Matsuno et al. 2006). However, the total area of paddy fields has been decreasing in recent years owing to urbanization, increasing area of fallow fields, and rice-yield controls imposed by the government. The rice yield has been controlled in Japan since the 1970s by a rotation of paddy rice with vegetables, wheat and soybean. In recent years, of the paddy-upland crop rotation has been conducted at the around 30% of total paddy fields. The decrease in paddy field areas has likely caused a decrease in the amount of groundwater recharge and decline of the groundwater level (Sugio et al. 1999; Watanabe et al. 2002; Khan et al. 2010). Clarifying the extent to which the decline in paddy field area affects the groundwater level is important to maintaining sustainable groundwater use. Although various studies have been carried out to examine groundwater flow and recharge from paddy fields (Elhassan et al. 2001; Chen and Liu. 2002; Chen et al. 2002; Anan et al. 2007), the effects of land use conditions, in particular paddy fields and crop-rotated areas, on groundwater recharge and groundwater level remain unclear. Groundwater recharge fluctuates both temporally and spatially because of various factors, such as soil permeability, land use conditions, topography, amount of precipitation, and timing of snowmelt. In addition, groundwater recharge from irrigated paddy fields depends on the soil structure and irrigation management. Soils in paddies are typically puddled before transplantion of the rice seedlings, to reduce percolation losses owing to decreases in the hydraulic conductivity of paddy soils. As a result, paddy soils present stratified layers that consist of the top puddled layer, muddy layer, plow sole (also, known as hardpan) layer, and underlying subsoil layer (Liu et al. 2001; Tournebize et al. 2006). Several paddy irrigation management methods are conducted in accordance with the growth stage of rice, including puddling, mid-summer drainage, and intermittent irrigation. Consequently, many factors influence groundwater recharge from paddy fields, such as top and subsoil thickness, hydraulic conductivity of plow sole layer, ponding water depth and soil puddling intensity (Chen and Liu 2002; Kukal and Aggarwal 2002; Lin et al. 2013).

Apart from groundwater recharge, there are several non-negligible factors that influence groundwater level, such as groundwater use (for drinking water, industrial water and for melting snow on roads) and interaction of the aquifer and rivers. Accordingly, it is necessary to assess the effects of natural and artificial

factors on temporal and spatial changes in groundwater flow and level. Numerical simulation is an effective analysis tool for assessment of these factors and attempts to integrate components of a hydrogeological system, climatic effects, and anthropogenic issues. Estimation of the groundwater recharge serving as the upper boundary of this simulation model is important to construction of a reliable model. Because groundwater recharge consists of water that reaches the groundwater body after moving through the unsaturated (vadose) zone, field measurements have difficulty in accurately evaluating the groundwater recharge. For paddy fields, the recharge is typically estimated using water balance methods (Bhadra et al. 2013; Don et al. 2006), tank models (Elhassan et al. 2001; He et al. 2008; Raneesh and Thampi 2013), and one-dimensional (1-D) unsaturated-zone flow analysis (Bogaard and van Asch 2002; Kaushal et al. 2009; Tournebize 2006; Xu et al. 2012). Combination of physically-based models for both the unsaturated and saturated zones has been employed in a number of studies. Lateral water flux is much lower than vertical water flux in agricultural fields (Chen et al. 1994; Zhu et al. 2012); therefore, an couple 1-D unsaturated-zone flow models with groundwater flow models is alternative method to simulate groundwater level (Šimůnek and Bradford 2008; Twarakvi et al. 2008). However, when coupled unsaturated-saturated zone models are applied to paddy fields, problems may arise because such models may not completely represent the characteristics of the fields or address complicated irrigation water management strategies. In the study area, fluctuations of groundwater levels at the beginning of the irrigation period are closely linked with the area of paddy fields around wells (Iwasaki et al. 2013a). Some researchers have examined the interaction between groundwater and river water in the area, including both river water infiltration to groundwater and groundwater flow to the river through hydrological and water quality observations (Tsuchihara et al. 2010; Futamata et al. 2005; Tsujimoto et al. 2005; Morita et al. 2008; Iwasaki et al. 2013b). Maruyama et al. (2012; 2014) estimated water balance in this area. Iwasaki et al. (2013b) performed steady numerical analysis considering the observed groundwater level contour maps and the measured interaction of water flowing between the aquifer and the river. Nevertheless, no feasible research has been carried out for transient analysis of groundwater environments in recent years in the study area.

Therefore, this study was conducted to determine the quantitative effects of different land use conditions, such as paddy and upland fields (including crop-rotated paddy fields) on the groundwater recharge and groundwater level in the Tedori River alluvial fan. To accomplish this, a steady state model was extended to a transient model that consists of a 1-D unsaturated zone model (HYDRUS-1D) for estimation of groundwater recharge and a 3-D groundwater model (MODFLOW). Based on groundwater flow simulation from 1975 to 2009, evaluation of relationships between changes in groundwater levels over time and changes in artificial or

natural factors was then performed.

2. Materials and Methods

2.1 Study Area

The study site is the Tedori River alluvial fan in Ishikawa Prefecture, Japan (Figure 1). The center of the fan is at North 36° 31′, East 136° 34′ (WGS 84). The alluvial fan was formed by the Tedori River and has the topographical shape typical of alluvial fans. The right side of the fan is wider than the left because the northeast area overlaps with the Sai River and the Asano River alluvial fan (Hokuriku Regional Agricultural Administration Office, 1977). The study area is on the right side of the fan, bounded by the Tedori River to the south, the Sai River and the Fushimi River (a branch of the Sai River) to the northeast, the Sea of Japan to the west, and the Hakusan mountains to east. The northeast boundary is hereafter referred to as the Sai River. The study area is about 16 km from north to south and 12 km from west to east, covering a total of about 140 km^2. The top of the fan is about 80 m above sea level (asl) and the average slope is 1/140 (the fan is relatively steep).

The study area is located in a humid region with a monsoon-dominated climate. According to meteorological observation data for 30 years (1981–2010) collected at the Kanazawa meteorological station 2 km east of the study area, the average annual precipitation and annual snow depth are 2399 mm and 281 cm, respectively, and the average annual temperature is 14.6 °C. Monthly precipitation from December to February is relatively high owing to the snowfall that occurs during this period. However, snowfall is likely to be decreased by the slight temperature rise expected for the region as a result of climate change (Japan Meteorological Agency, 2008). In addition, river water flow decline (Noto et al. 2013a; 2013b) or an increase in sea level due to climate change may also affect groundwater conditions. The rice irrigation period, when irrigation water is allocated from the Tedori River, is from mid-April to early September in the study area. Rice is planted at the beginning of May and a mid-summer drainage is conducted during June to temporarily dry the paddy fields, after which intermittent irrigation is conducted. In paddy fields, growers typically adopt the rice-upland crop rotation of soybeans and barley seeds, with soybean grown in the summer (from June to October) and barley in the winter (from November to May).

2.2 Hydrogeology

Figure 2 illustrates the hydrogeological conditions across the study area. The main geological deposit is sandy gravel with a depth of over 130 m in the middle of the fan. In the middle and upper parts of the fan, the aquifer

is confined by alluvium composed of alternate layers of sandy gravel (diluvium and alluvium) and sandy gravel and clay (Quaternary and Tertiary) (Hokuriku Regional Agricultural Administration Office, 1977). Underlying the alluvium is Tertiary bedrock. Along the coastline of the Sea of Japan, a clay layer is wedged into the gravel layer. In this study, the sandy gravel layer and the sandy gravel and clay layer are regarded as aquifer materials and were modeled as the shallow and deep aquifer, respectively.

2.3 Land use

Paddy fields are the dominant land use in the study area. Land use data (100-m grid) are available from the National Land Numerical Information download service (the Ministry of Land, Infrastructure, Transport and Tourism, 2011). The paddy field area ratio (paddy field area/total area) was 70%, 62%, 61%, 58%, 52% and 45% in 1976, 1987, 1991, 1997, 2006 and 2009, respectively. The land use of the area in 2009 consisted of paddy, upland, urban (building), river, and other land covering 45%, 2%, 39%, 4%, and 10% of the total, respectively. There has been great expansion of urban areas in Kanazawa, the prefectural capital, which is located on the northeast portion of the fan. There are also many business entities in this area of the fan (e.g., food factories, breweries, and precision machine factories), which require a high volume of clean groundwater. The upland field ratio is about 2%, and this has changed very little over time. Fields in this area are primarily distributed in the coastal zone near the Sai River. The area of urban land has increased considerably around the central part of Kanazawa and along Route 8. The increases in urban land have been almost equal to decreases in paddy field area. The rate of paddy rice-upland crop rotation in the study area increased from 4.9% in 1976 to 25.4% in 2009. Since 1998 the rates have fluctuated between 25% and 33%.

2.4 Groundwater use

Annual groundwater use in the fan was 1.0×10^9 m^3/y in 2008 (Ishikawa Prefecture, 2010), of which industrial, drinking, ‘snowmelt’, irrigation, and building maintenance water accounted for 59%, 30%, 4%, 4%, and 3%, respectively. Groundwater for snowmelt is groundwater applied to the road in order to melt freshly fallen snow on the road by ejecting groundwater (sometimes artificially heated) through pipelines laid under the road (Kayane, 1980), which means that groundwater is used as heat energy for snowmelt. The monthly groundwater use in 2005 was highest in December because large amounts of groundwater are used for melting snow, while the lowest use was in November. The drinking water supply systems in Kawakita and Nomi depend solely on

the groundwater. In addition, 99% of the drinking water is supplied by deep wells from the confined aquifer (Ishikawa Prefecture 2012). According to the spatial distribution of annual groundwater use (1-km grid) in 1987, 1993, and 2008, the amount of groundwater use is large in the downstream section of the Tedori River and in central parts of Kanazawa. Annual groundwater use increased until 1992 because of increasing drinking water requirements, but showed little change from 1992 to 2009 owing to regulation of groundwater overdraft (Ishikawa Prefecture 2010).

2.5 Groundwater environments

Groundwater levels have been monitored continually at 11 sites with 13 monitoring wells (wells A-K in Figure 1) in Tedori alluvial fan. Seven of these wells (C-I wells in Figure 1) are located within the study area. The groundwater levels have been monitored with automatic pressure type or float type water-level gauges since 1974 (with some exceptions), with 3-hour interval groundwater levels averaged every 24 hours.

The groundwater-level contours were obtained from mapping and kriging of groundwater levels in the fan, which were observed temporally at 113 wells in December of 1993, 87 wells in November of 2009, and 86 wells in June of 2010, which are used ordinarily. Comparisons of the groundwater levels during the irrigation period in 2010 and the non-irrigation period in 2009 show that water level during the irrigation period was 5 m higher than that of the non-irrigation period. Additionally, the groundwater level during the non-irrigation period declined 5 m over 17 years (from 1993 to 2009). The groundwater-level contour maps showed that the groundwater flows from the upper zone of the fan to the northwest side, and flow lines perpendicular to contours point in the downstream direction, indicating that they are controlled by the topographic gradient of the land surface and seepage water from the Tedori River. Lateral flow from the mountain front is not observed in the study area judging from the groundwater-level contour maps. Additionally, there was no clear evidence of the lateral flow based on several spatial distributions of ions, elements, and stable isotopes of water and strontium of groundwater.

To determine groundwater–river water exchange volumes, river flow amounts at eight points along the Tedori River and inflow amounts entering the river (10 points) were measured, after which the amount of water flowing from the river to groundwater or from groundwater to the river in each interval was calculated considering a water balance between the neighboring observation points. The measurements were conducted in the irrigation (2009 June) and non-irrigation (2009 December) periods. The measurement range was from 1.1 to 16.4 km from the river mouth. The obtained results indicated that a large amount of seepage water recharges to

the riparian groundwater section at 2.2–16.4 km from the river mouth (during the irrigation period: 4.1×10^6 m^3/d, during the non-irrigation period: 5.1×10^6 m^3/d), and that groundwater flows to the river in the downstream section at 1.1–2.2 km (during the irrigation period: 1.1×10^6 m^3/d, during the non-irrigation period: 7.5×10^5 m^3/d). These measurement data were used to calibrate the groundwater model introduced in the next section.

2.6 Summary of the analysis

In this study, groundwater recharge was calculated with the HYDRUS-1D 1-D unsaturated-zone flow model and adapted to the upper boundary condition of the MODFLOW 3-D groundwater flow model. Recharge areas were set as the paddy field and upland field, including crop-rotated paddy fields. Other land use conditions were considered as non-recharge areas. MODFLOW's domain arrays were identified as calculation cells. Each unsaturated soil profile was set for each calculation cell assigned to recharge area. The bottom water flux at each calculation cell in the recharge area was determined by HYDRUS-1D under a time variable atmospheric boundary condition.

3. Unsaturated Zone Flow Model

3.1 Governing equations

Water movement in the unsaturated zone was assumed to occur only in the vertical direction, which is described by a modified form of the Richards equation:

$$\frac{\partial\theta}{\partial t}=\frac{\partial}{\partial z}\left[K\frac{\partial h}{\partial z}+K\right]-S \tag{1}$$

where θ is the volumetric soil water content, which is a function of the pressure head for a given material (dimensionless), t is time (T), z is the vertical coordinate (L) (positive upward), K is the unsaturated-zone hydraulic conductivity at the current pressure head (L/T), h is the water pressure head (L), and S is the sink term by plant roots (1/T).

The unsaturated soil hydraulic properties, θ and K, are highly nonlinear functions of the pressure head. In this study, the hydraulic properties were calculated using the equations described by van Genuchten (1980). The soil water retention, $\theta(h)$, and hydraulic conductivity, $K(h)$, functions are given by:

$$\theta=\frac{\theta_s-\theta_r}{\left[1+\left|\alpha h\right|^n\right]^m}+\theta_r\ (h<0),\ \theta=\theta_s\ (h\geqq 0) \tag{2}$$

$$K(h) = K_s S_e^l \left[1-(1-S_e^{1/m})^m\right]^2 \quad (3)$$

$$S_e = \frac{\theta - \theta_r}{\theta_s - \theta_r} \quad (4)$$

where n is a pore-size distribution index (dimensionless) (m=1-1/n, n >1), l is a pore-connectivity parameter (dimensionless), α is the inverse of the air-entry value [1/L], θ_r is the residual water content (dimensionless), θ_s is the saturated water content (dimensionless) and S_e is the effective water content (dimensionless). The pore-connectivity parameter l in the hydraulic conductivity function is estimated to be about 0.5 for many soils (Mualem 1976). Five parameters (K_s, θ_s, θ_r,α, n) are required for the calculations.

The numerical model used was Version 4.0 of HYDRUS-1D, a software package for simulating water, heat, and solute movement in one-dimensional variably saturated media based on finite element representation of the governing equations (Šimůnek et al. 2008).

3.2 Model discretization

The soil profiles were set from the soil surface to 5 m below the water table considering the fluctuation in groundwater level. The depth of the water table was determined from the difference between ground surface elevation and interpolated groundwater levels during the non-irrigation period in 1993 (Figure 3(b)). The depth varied from 2 m to 45 m, and was deeper in the upper region of the fan than the lower region. The soil profile was vertically discretized into two layers. The upper layer, from the surface to 0.3 m depth, was the low permeability layer (plow sole), which occurred under the puddled top soil. The plow sole is the major factor controlling the infiltration rate and groundwater recharge in paddy fields (Chen et al. 2002). The lower layer, from 0.3 m depth to the bottom of the vertical calculation domain, was the subsoil under the plow sole. As shown in Figure 3(c), the hydraulic parameters were initially grouped into three zones considering the shallow aquifer zoning (described in detail below). Parameters of the soil water retention curve were calibrated to fit the groundwater fluctuation. Optimized parameters are shown in Table 1. Optimized saturated conductivities of the plow sole layers were relatively large. This reason is explained as follows. Soil water flows in unsaturated condition in an open system with negative pressure because the soil surface infiltration is given by prescribed water flux (Table 2) and depths of groundwater level are around 5–40 m (Figure 3(b)). The unsaturated zone conductivity becomes low significantly under the unsaturated condition. The groundwater recharge (bottom flux) at the rice-planted paddy fields was simulated reasonably (as mentioned below). Optimized saturated zone conductivity is therefore nothing more than one parameter to determine the shape of the unsaturated-zone

hydraulic conductivity function based on the van Genuchten-Mualem model.

The recharge areas were paddy and upland crop-rotated paddy fields. Buildings and roads constitute possible land uses for the recharge area, apart from the agricultural fields. However, roads are regarded as impermeable because they are usually made of asphalt. The ratio of the floor space to the total building space is around 33 % in Kanazawa City. When about two-thirds of the building field was set as the recharge area, the simulated groundwater-levels had lower reproducibility of the seasonal fluctuations than simulations of the building field set as totally impermeable area. Thus, land use conditions other than agricultural fields were considered as non-recharge areas. For each year, a cell was assigned as either a paddy cell, upland cell, or a non-recharge cell as follows: all cells were ranked in ascending order according to the paddy field area ratio in each cell. The cells having larger paddy field area ratios were then specified to be uniform paddy field cells in decreasing order. The number of specified paddy cells was set so that the sum of their areas was equal to the actual paddy field area. A similar method was used to determine the upland cells. The cells specified as neither paddy cells nor upland cells were set as non-recharge area cells. Among the paddy cells, the crop-rotated paddy cells were randomly reconfigured considering the rate of paddy rice-upland crop rotation in each year and assuming that the rotation was not carried out for two years running. Figure 3(a) shows the recharge area in 2009. Temporal variations for the paddy and upland field areas were obtained using a linear interpolation method and land use data available in 1976, 1987, 1991, 1997, 2006 and 2009. The rate of paddy rice-upland crop rotation in this area was available for each year. Land use conditions were changed from November considering the cropping schedule for each year (one hydrological year in this study was from November to October).

3.3 Boundary conditions and input data

The upper boundary condition was set to be a time variable atmospheric boundary condition and the lower boundary condition was set to be a free drainage condition because of the deep water tables. Details of numerical coupling methods concerning the unsaturated zone model's boundary conditions have been reported by Furman (2008). HYRDUS-1D requires precipitation, potential evaporation, and potential transpiration data, which were obtained from the Kanazawa meteorological station for the present study. Potential evapotranspiration was calculated according to the Penman method. Monthly albedo for paddy and upland fields were based on Kotoda (1989). Potential evapotranspiration was partitioned into an evaporation

component and a root water uptake component (transpiration). Potential transpiration rates, *T*, were derived from the following equation (Campbell, 1985):

$$\frac{T}{ET} = 1 - \exp\left(-0.82\mathrm{LAI}\right) \tag{5}$$

where, LAI is the leaf area index defined as the total one-sided leaf area per unit ground area (dimensionless). In this study, LAI was multiplied by the vegetation cover ratio (defined as the percentage of area covered with plants per ground area) considering the furrow area. A month is divided into three parts (decade days): early of month (10 days), middle of month (10 days), and end of month (remaining days). Values of LAI were derived on a decade days basis for rice, soybeans, and barley seeds using values reported by Shibayama et al. (2011), Shimada et al. (1990), and Takeda and Udagawa (1976), respectively. Values of the vegetation cover ratio for soybeans were obtained on a decade days basis from Satoh (2002), while those for rice and barley seeds were estimated using an empirical model between the vegetation cover ratio and LAI by Nakamura et al. (2007) and Fukushima et al. (2003), respectively.

Water extraction in the root zone was calculated from the potential transpiration and root-length density by the Feddes root water uptake model (Feddes et al. 1978). Root water uptake parameters of the Feddes model for soybean and barely were used as database values of HYDRUS-1D, while those reported by Phogat et al. (2010) were used for rice. The depth of the root zone was 0.2 m below the soil surface and the root-length density in the root zone was assumed to be uniformly distributed.

The initial conditions were considered to be a uniform pressure head (-1 m) throughout the vertical soil profile. Leterme et al. (2013) indicated that relatively long warm-up periods were necessary to avoid oscillations of calculation (at least several years), even while the numerical solution eventually stabilized. This was partly due to the presence of zones with a deep water table, which resulted in atmospheric input taking several years to migrate through the unsaturated zone. Since Lererme et al. (2013) used a warming-up period of 10 years to ensure results independent of the initial conditions, the same warming-up period was used in this study. During the warming-up period, weather data from November 1975 to October 1976 were used because the weather data in this duration were similar to the averaged value during 1980-2010.

According to Noto et al. (2013), snowmelt water amount was calculated by the following model to the Tedori River basin:

$$S = m_s T + \frac{RT}{80} \tag{6}$$

where, *S* is the daily snowmelt (L/T), m_s is the snowmelt coefficient (L/(°C T)), *R* is the daily precipitation (L/T),

and T is the daily mean temperature (°C). The coefficient m_s was estimated to demonstrate short-term groundwater fluctuations by trial and error (m_s=7 mm/(°C d)). Snowmelt was set to 0 mm when snowfall was observed and the degree-day model was used when snowfall was not observed. Snowfall data used were obtained from the Kanazawa meteorological station. Evaporation at the surface was not considered during application of the model because the model considers snowmelt at the snow surface based on evaporation.

Since HYDRUS-1D does not include an irrigation management model, some irrigation scenarios were set that considered both the observed irrigation practices and volume of water rights for puddling purposes in the study area. Table 2 summarizes the paddy irrigation management settings. The maximum ponding depth for paddy fields was set at 0.15 m during the irrigation period, while that of upland fields (including crop rotated fields) and paddy fields during the non-irrigation period was set at 0.03 m.

HYDRUS-1D was run using daily stress periods. Decade-days recharge values were derived by averaging daily recharge values from HYDRUS-1D and used for the upper boundary condition for the groundwater flow model to reduce computational efforts.

4. Groundwater Flow Model

4.1 Governing equations of groundwater flow

A 3-D centered finite difference numerical model was developed based on MODFLOW 2005 (Harbaugh 2005). The MODFLOW series (Harbaugh and McDonald 1996; Harbaugh et al. 2000; Harbaugh 2005) developed by the United States Geological Survey is the most reliable among existing groundwater models. Considering mass balance law of water and the Darcy's gradient type relationship, the governing equation for the 3D groundwater flows for isotropic aquifers is:

$$S_s \frac{\partial h}{\partial t} = \frac{\partial}{\partial x}\left(K_s \frac{\partial h}{\partial x} \right) + \frac{\partial}{\partial y}\left(K_s \frac{\partial h}{\partial y} \right) + \frac{\partial}{\partial z}\left(K_s \frac{\partial h}{\partial z} \right) + q \tag{7}$$

where, K_s is the saturated hydraulic conductivity (L/T), h is the potentiometric head (L), S_s is the specific storage of the porous medium (1/L), and q is the flux per unit volume representing sources and/or sinks of water; $q > 0$ for inflow and $q < 0$ for outflow, and x, y, z are coordinate (L).

4.2 Model discretization

In MODFLOW, an aquifer system is approximated as a discretized domain that consists of an array of nodes

and associated finite difference blocks (cells). A schematic sketch of the grids and layers used in this study is shown in Figure 3. The model domain was discretized into grid dimensions of 400 m × 400 m. Overall, the model contained 897 cells for each layer and four layers, giving a total of 3,588 cells. The first to third layers represented the shallow aquifer, and a part of the second layer included the coastal clay zone. The fourth layer represents the deep aquifer. The surface elevation of the upper layer was derived from digital elevation model (DEM) data with a ground resolution of 50 m, while the bottom of the fourth layer was defined horizontally at -200 m from sea level. The second and third layers were determined based on information derived from borehole geological data (Hokuriku Regional Agricultural Administration Office 1977).

4.3 Boundary conditions and input data

The model was calibrated under both steady state and transient state conditions. Steady state calibration was conducted to determine the hydraulic conductivities and hydraulic conductance of riverbed materials. Transient state simulation was optimized by adjusting the storage coefficients. These calibrations are explained in the following sections.

4.3.1) Steady state simulation

To estimate hydraulic conductivities, steady state calibration was first carried out under the following conditions. To consider the spatial distribution of the hydraulic conductivity over the shallow aquifer, cells in layer 1 were grouped into three zones (northern, southern and coastal) based on the surface geology. The same zones were also applied to layers 2 and 3. The part of layer 2 corresponding to the coastal clay zone had different hydraulic properties. Layer 4 (deep aquifer) was not divided. The zone settings are shown in Figure 3(c). Overall, five hydraulic parameter zones were set up. A no flow boundary condition was applied to the eastern mountain-front boundary of aquifers and the bottom of the model domain. Constant head boundary conditions were set along the rivers (the Tedori River and the Sai River) using interpolated measured groundwater heads (2010 June) and the Sea of Japan using the mean sea-level surface. The sea-level surface at Kanazawa Bay is available in NOWPHAS (Ministry of Land, Infrastructure, Transport and Tourism, 2011). Internal boundary conditions such as rivers and lakes, which significantly influence groundwater, do not exist in the study area. The recharge flux, which is specified as the upper boundary condition, was calculated from field measurements of the paddy water percolation rate. Murashima (2009) investigated the 12-hour interval water requirement rate in 36 paddy plots in the fan from 11 May to 10 August 2008 and calculated the daily water requirement with depth. The mean water

requirements were 15.6 mm/d before and 24.7 mm/d after the mid-summer drainage, and standard deviations of the water requirements after the drainage were larger than before the drainage. The mean water requirements before and after the mid-summer drainage did not differ significantly at a P-value of 0.05 between the three zones associated with the hydraulic conductivities of the model domain. Water percolation rates before and after the mid-summer drainage, which were calculated by subtracting the evapotranspiration during the irrigation period from the mean water requirement, were 7.4 mm/d and 10.9 mm/d, respectively. All of the percolated water supplied to the aquifer was considered to be in steady state during the irrigation period (Maruyama et al. 2014). Considering paddy rice-upland crop rotation, the recharge fluxes were calculated as the percolation water rate (7.4 mm/d) and multiplied by both the paddy field area ratio in each cell and the area ratio of rice-planted fields to paddy fields. Groundwater use data for each cell were created considering the spatial distribution of annual groundwater in 2008 and the monthly ratio of groundwater use in June (Irrigation period) to annual groundwater use (8.1%).

A steady state calibration for the hydraulic conductivities of five zones was performed by trial and error and the inverse method using PEST (Doherty 2004). PEST automatically adjusts model parameters until the fit between model outputs and observations is optimized. In this study, the observed data consisted of groundwater levels during the irrigation period (2010 June) at 38 wells for which the depths of strainers or well bottoms were known. The results of the optimized hydraulic conductivities are shown in Table 3. The conductivities of the shallow aquifer (southern zone) and deep aquifer from pumping tests were 4.0×10^{1} m/d and 1.7×10^{0} m/d, respectively. Okuyama (2011) reported that the conductivity of the shallow aquifer (northern zone) from a laboratory permeameter test was 2.3×10^{2} m/d. The calibrated results were sufficiently close to the estimated values from the field and laboratory tests. The mean error between the simulated and measured (ME) groundwater levels was 0.9 m, while the root mean square error (RMS) and normalized RMS (NRMS) were 2.1 m and 3.3%, respectively. Groundwater level contours from the simulated heads agreed with those of the observed levels in June of 2010. Overall, the developed model simulated the observed results reasonably well.

To calculate the water exchange between the Tedori River and the aquifer, a second steady-state calibration was carried out by taking into account head-dependent boundary conditions using the MODFLOW river package (Harbaugh 2005). The groundwater is hydraulically connected to the river if the water table is above the elevation of the base of the streambed sediments of the river. In this case, the river package calculates the recharge through the river bed using the following equation:

$$Q = C\left(H - h\right) \tag{8}$$

where Q is the exchange flow between the groundwater and river water (L^3/T), C is the hydraulic conductance of the riverbed (L), and H is the river surface level (L). The conductance is calculated from:

$$C = \frac{K_r LW}{M} \tag{9}$$

where L is the length of a reach through a cell (L), W is the width of the river in the cell (L), M is the thickness of the riverbed (L) and K_r is the vertical hydraulic conductivity of the riverbed material (L/T).

In this study, data describing the river levels and width of the river were obtained from observation of the flow of the Tedori River in June 2009. The recharge through the river bed was calculated using equation (9) under the assumption that the thickness of the riverbed was 15 m. The vertical hydraulic conductivities of the riverbed materials were determined so that water flow from the river to the groundwater, which is calculated in the second model calibration, was equal to that calculated in the first model calibration.

In the section along the river in which groundwater flowed into the river, the constant head boundary was specified.

The ME, RMS and NRMS were 0.9 m, 2.1m and 3.4%, respectively. The contours of simulated groundwater heads agreed well with those of the observed heads. The calculated exchange flow between the groundwater and the right bank of the river was 43% of the total observed exchange flow, which does not contradict the observed results; therefore, the model calibration result is considered reasonable.

4.3.2) Transient state simulation

Specific coefficients were determined by a transient state calibration. The hydraulic conductivities and conductances, which were estimated from the steady state calibration, were used in the transient calibration. The transient simulation spanned a 35-year period (1975-2009) and the storage coefficients were assigned based on the hydraulic conductivity zones.

Along the Sai River and downstream section of the Tedori River, constant head boundary conditions were set using interpolated water levels in December of 1993 (non-irrigation period) because groundwater levels near these sections changed only slightly both seasonally and over the long term. Other boundary conditions were the same as those in the above second steady state calibration. This can be justified because of the small changes in river water levels in the Tedori River and mean sea level at the Sea of Japan during the simulation period.

Fine spatial and temporal distributed groundwater use data were not available. Accordingly, datasets with monthly intervals for the period from 1975 to 2009 were created considering the spatial distribution of the

annual groundwater in 1993 and temporal variation of annual and monthly groundwater use in 2005. Monthly-based groundwater use in each cell was applied for the transient groundwater flow simulations.

The map of groundwater levels in December of 1993 was used to set the initial heads for the transient state calibration. The computational time step was set as one day. The groundwater levels in the eight monitoring wells (wells C-I in Figure 1) were used for model calibration. Optimized storage coefficients are shown in Table 3.

5. Results and Discussion

5.1 Seasonal and annual changes in groundwater level

Figure 4 shows a comparison of the decade-average of the calculated and observed groundwater levels in well D. The seasonal pattern of fluctuation was reasonably reproduced. Initially, there was a substantial increase in the groundwater level from the end of April to early May (the beginning of the irrigation period) due to paddy fields being plowed and irrigated before transplantation of the rice seedlings. From July to September (the irrigation period), groundwater levels remained high and stable. From September to October (the beginning of the non-irrigation period), groundwater levels decreased dramatically. Finally, during November to April (the non-irrigation period), groundwater levels fluctuated in response to precipitation, snowfall, and snowmelt. The increase in groundwater levels at the beginning of the irrigation period is considered to be typical of groundwater level changes in the paddy irrigation area (Horino et al. 1989; Imaizumi et al. 2006). Overall, the model was able to reasonably compute seasonal fluctuations, which were significant in response to paddy irrigation such as the increase of groundwater levels at the beginning of the irrigation period. Other observation wells also showed fluctuations with the difference in the degree of increase of groundwater levels. Figure 5 shows comparisons of the calculated and observed groundwater-level contour maps. The observed groundwater-level contours were based on simultaneous observations of groundwater level in early December 1993, mid-November 2009, and early June 2010. Because the simulation period is until November of 2009, the simulation results did not provide the contours in November of 2009 and June of 2010. The contours in November of 2008 and June of 2009 were used instead of those of November of 2009 and June of 2010. Simulated groundwater levels were averaged for decade days and shallow simulated groundwater-level contours approximately fit the observations of the three periods.

There were some differences between the predicted and the observed results. Specifically, the absolute values between the observed and calculated groundwater levels varied. This was partly due to the

resolution of the MODFLOW cells (400 m × 400 m). There were also sluggish decreases in calculated groundwater levels after the irrigation period. Namely, there was a lag time in groundwater recharge because the groundwater depth was relatively deep and the infiltration water did not contribute to the groundwater recharge promptly. Moreover, temporal and local groundwater changes in winter did not respond to groundwater use for melting snow because of lower-resolution input data in space (based on a 1-km grid) and time (monthly). Figure 6 shows the observed groundwater levels at wells E, F, I, and H. The lowest decade-averaged groundwater level was observed in the 1990s, while the groundwater levels increased slightly during the 2000s, probably because of a reduction in annual groundwater use. However, the lowest calculated value was in the 2000s, which was likely due to the low spatial and temporal resolution of the groundwater use setting. Based on the above results, this model could calculate changes in groundwater reasonably, despite the limitations of the model structure and data. The ME, RMS and NRMS were 0.5 m, 1.8 m and 5.4%, respectively.

The fan was divided into 6 zones with approximately equal area, which are shown in Figure 7. Figure 8 shows the average calculated groundwater level in each zone. The decreasing trends of groundwater levels in each zone were similar to temporal changes in some observed wells (Figure 6). Groundwater levels averaged over the hydrological year (from November to October) declined from 1975 to 2009, with a maximum decrease of 3.5 m being computed in zone 1. Change rates of groundwater levels averaged over the hydrological year or the irrigation period (from mid-April to early September) are shown in Table 4. Positive values indicate the rate of groundwater increase, while negative values indicate groundwater depression. In zone 1 (the upper zone of this fan) and zone 2 (the middle zone of this fan, near the Tedori River), the groundwater levels decreased by an average of -0.07 m/y, which was larger than in other zones. During the irrigation period, the greatest rate of decrease was -0.10 m/y in zone 2, and relatively small values are -0.08 m/y in zone 1 and 4. The annual changes in groundwater levels caused by changing the paddy field area were more affected by changes in the paddy field area in the middle part of the fan. One reason for this is that the groundwater catchment area is limited in the upper and middle part of the fan relative to the lower part.

5.2 Seasonal changes in groundwater recharge

Figure 9 shows the mean of seasonal precipitation, snowmelt water, evaporation, transpiration and groundwater recharge from the paddy and upland fields, including the rotated paddy fields, over 35 years and the standard deviations. The recharge value at the paddy fields was relatively large (average, 10.2 mm/d) from early May to

early June owing to the beginning of paddy irrigation. The averaged recharge values in the period influenced by the mid-summer drainage (mid-June to early July) and after that period (mid-July to the end of August) were 6.5 mm/d and 10.8 mm/d, respectively. Maruyama et al. (2014) estimated the water percolation to be 10.7 mm/d in 2008 by subtracting evapotranspiration from the water requirement rate observed during mid-May to early August and by weighting by days after and before the mid-summer drainage. The ratio of calculated recharge to water percolation was 90%. Measured water percolation may contain water components that do not contribute to groundwater recharge such as the volume of water that flows to the sea. These findings suggest that the groundwater recharge estimated using HYDRUS-1D had reasonable precision. The recharge amounts in the non-irrigation period from both paddy and upland fields were relatively high in the snowfall and spring snowmelt periods, with the largest value of 5.8 mm/d being observed from early to mid-March. The average recharge from mid-September to the end of November, which accounts for 35% of the rainfall, is 1.1 mm/d and the groundwater level is approximately constant.

The annual recharge in the hydrological year from the paddy and upland fields was 1819±202 mm and 886±287 mm, respectively. The total recharge during the irrigation period from the paddy and upland fields was 1207±57 mm and 220±106 mm, respectively. The annual recharge at the upland field was mean 36 % of the annual precipitation. In paddy fields, the ratio of the irrigation period to a year was about 74%. Taken together, these findings indicate that irrigated rice-planted fields have a 5.5-fold greater ability to recharge groundwater than upland fields.

5.3 Annual changes in groundwater recharge

The annual net water balances for 35 years were calculated considering the study area as a groundwater basin (Figure 10). Both the Tedori River (the head-dependent boundary) and the surface boundary were net inflow sources, and the ratios for total net inflow were 30% and 70%, respectively. Net outflow sources were groundwater use and outflows to the sea and the Sai River (the constant head boundary), and the ratios for total net outflow were 40% and 60%, respectively. These results suggest that the groundwater recharge from agricultural fields has a greater effect on groundwater levels than groundwater use.

Figure 11 shows the annual changes in precipitation and the agricultural area ratios, as well as the recharge for the entire model domain. Groundwater recharge is divided into two recharge fields, rice-planted paddies and upland (including rotated) paddies. Ratios of each agricultural (paddy, rice-planted paddy, and

upland) area to the total study area are shown. Ratios of rice-planted paddies to total groundwater recharge ranged from 80% to 96%, indicating that rice-planted paddies are the dominant groundwater recharge source. The ratio of paddy area (including the crop rotation) and rice-planted paddy area decreased by 34% and 48%, respectively, from 1976 to 2009. Total recharges at rice-planted paddies and upland paddies ranged from 7.17×10^7 in 2008 to 1.95×10^8 in 1977 and from 6.13×10^6 in 1976 to 2.89×10^7 in 1983, respectively. Regional groundwater recharges ranged from 7.93×10^7 in 2009 to 2.03×10^8 m^3 in 1977. Under the influence of decreased rice planted paddies and precipitation, the amount of regional groundwater recharge is decreasing, with a total decrease to 61% of the peak in 1977. The Mann-Kendall test ($P = 0.05$) revealed that agricultural area ratios (rice-planted, paddy and upland fields), precipitation, snowfall, and groundwater recharge from 1975 to 2009 showed significantly decreasing trends. There was no change in the rate of paddy rice-upland crop rotation and groundwater use.

Groundwater storage was estimated from annual average groundwater levels and effective porosities. Effective porosities were used to determine the approximate specific yield (Table 3). The average groundwater storage was 2.9×10^9 m^3 over 35 years, with a decrease of 2.4×10^7 m^3 occurring from 1976 to 2009. The annual groundwater recharge was comparable to about 4.8% (from 2.8% to 7.0%) of groundwater storage. The influence of rice-upland crop rotation on groundwater recharge was evaluated by simulation using the hypothetical land use scenario without paddy rice-upland crop rotation. The simulation revealed that the groundwater recharge would decrease to 5–32% for paddy fields and 2–27% for the whole model relative to no crop rotation system. Under ‘no crop-rotation’ systems, change rates of groundwater levels for each zone ranged from -0.02 to -0.05 m/y, with a maximum drawdown of 1.3 m occurring from 1975.

The decrease in groundwater storage over 35 years was 1% of the total storage. However, groundwater recharge was 5% of the storage and 1.1–2.8 times the amount of groundwater use. Hence, it was confirmed that the conservation of paddy fields is of importance for sustainable groundwater use. Furthermore, the effects of the crop rotation on groundwater recharge were non-negligible; however, additional studies are warranted.

6. Conclusions

This study was conducted to develop a groundwater model that considered unsaturated zone flow to compute water-table fluctuations in the Tedori River fan in response to paddy irrigation management, rainfall, snowfall,

snowmelt, and evapotranspiration. The model consisted of the 1-D unsaturated-zone water flow model (HYDRUS-1D) for estimating groundwater recharge and a 3-D groundwater flow model (MODFLOW). The fine distribution of agricultural fields was modeled by coupling the 1-D unsaturated-zone flow model to the 3-D groundwater flow model through simulating groundwater recharge for each 3-D model grid (400 m×400 m). . This technique enabled spatial and temporal groundwater levels to be estimated reasonably and groundwater recharge to be estimated appropriately, although some improvements could be made to enable more accurate simulation. Noticeable results in the transient simulation during 1975 to 2009 were as follows:

(1) Annual groundwater recharge decreased over time. Regional groundwater recharges ranged from 7.93×10^7 in 2009 to 2.03×10^8 m^3 in 1977. The total amount of regional groundwater recharge decreased to 61% of the peak in 1977 because of declines in rice-planted field area and precipitation. Thus, groundwater levels have decreased to 3.5 m in the upper zone over 35 years.

(2) Irrigated rice fields have a 5.5-fold greater ability to recharge the groundwater than upland fields. The rice-upland crop rotation system could possibly decrease groundwater recharge to 2–27% relative to no crop rotation system.

Future studies should include quantitative assessments of the impact of predicted climate change or social change on groundwater recharge and groundwater levels using the developed transient model.

Acknowledgments

This research was supported by a subsidy from the Ministry of Agriculture, Forestry and Fisheries of Japan entitled “Normal hydrological cycle in the Tedori River Alluvial Fan areas as a core of irrigation water”. The authors thank the Ishikawa Prefectural government and Ishikawa Prefectural University for providing statistical datasets.

References

Anan M, Yuge K, Nakano Y et al (2007) Quantification of the effect of rice paddy area changes on recharging groundwater. Paddy Water Environ 5:41–47. doi:10.1007/s10333-006-0059-1

Bhadra A, Bandyopadhyay A, Sing R et al (2013) Develop of a user friendly water balance model for paddy. Paddy Water Environ 11:331–341. doi:10.1007/s10333-012-03244

Boggard TA, van Asch TWJ (2002) The role of the soil moisture balance in the unsaturated zone on movement

and stability of the beline landslide, France. Earth Surf Process Landforms 27:1177–1188. doi:10.1002/esp.419

Campbell GS (1985) Soil physics with basic transport models for soil-plant system. Elsevier, Amsterdam

Chen SK, Liu CW (2002) Analysis of water movement in paddy rice fields (I) experimental studies. J Hydrol 260:206–215.

Chen SK, Liu CW, Huang HC (2002) Analysis of water movement in paddy rice fields (II) simulation studies. J Hydrol 268:259–271

Chen Z, Govindaraju RS, Kavvas ML (1994) Spatial averaging of unsaturated flow equations under infiltration conditions over areally heterogeneous fields-1. Development of models. Water Resour Res 30(2):523–534

Doherty J (2004) PEST model - independent parameter estimation user's manual. Watermark Numerical Computing, Brisbane

Don NC, Hang NTM, Araki H et al (2006) Groundwater resources and management for paddy field irrigation and associated environmental problems in an alluvial coastal lowland plain. Agr Water Manage 84:295–304. doi:10.1016/j.agwat.2006.03.006

Eaneesh KY, Thampi SG (2013) A simple semi-distributed hydrologic model to estimate groundwater recharge in a humid tropical basin. Water Resour Manage 27:1517–1532. doi:10.1007/s11269-012-0252-5

Elhassan AM, Goto A, Mizutani M (2001) Combining a tank model with a groundwater model for simulating regional groundwater flow in an alluvial fan. Trans of JSIDRE 215:21–29

Feddes RA, Kowalik PJ, Zaradny H (1978) Simulation of field water use and crop yield, Simulation of field water use and crop yield, PUDOC, Wageningen, Simulation Monographs,189 pp.

Fukushima A, Kusuda O, Furuhata M (2003) Relationship of vegetation cover to growth and yield in wheat. Rep Kyusyu Br Crop Sci Soc Japan 69:33–35 (in Japanese)

Furman A (2008) Modeling coupled surface-subsurface flow processed: a review. Vadose Zone J. 7:741–756. doi:10.2136/vzj2007.0065

Futamata K, Takahashi I, Inoue M (2005) Influence of river stream on groundwater and recharge in the Tedori River alluvial fan areas. Research Report of the Hokuriku Regional Office, Ministry of Construction 209–212 (in Japanese)

Harbaugh AW (2005) MODFLOW-2005, The U.S. Geological Survey Modular Ground-Water Model - the Ground-Water Flow Process: U.S. Geological Survey Techniques and Methods 6-A16, Available via http://water.usgs.gov/nrp/gwsoftware/modflow2005/modflow2005.html. Cited 9March 2014

Harbaugh AW, Banta ER, Hill MC et al (2000) MODFLOW-2000, the U.S. Geological Survey Modular Ground-Water Model - User guide to modularization concepts and the ground-water flow process. U.S. Geological Survey Open-File Report 00-92, p. 121

Harbaugh AW, McDonald MG (1996) User's documentation for MODFLOW-96, an update to the USGS modular finite-difference ground-water flow model: USGS Open-File Report 96–485

He B, Takese K, Wang Y (2008) A semi-distributed groundwater recharge model for estimating water-table and water-balance variables. Hydrogeol J 16:1215–1228. doi:10.1007/s10440-008-0298-x

Hokuriku Regional Agricultural Administration Office (1977) Hydraulic geology and groundwater in Ishikawa prefecture (in Japanese)

Horino H, Watanabe T, Maruyama T (1989) Studies on the role of groundwater in water used for irrigation. Trans of JSIDRE 144: 9–6 (in Japanese with English abstract)

Imaizumi M, Ishida S, Tsuchihara T (2006) Long-term evaluation of the groundwater recharge function of paddy fields accompanying urbanization in the Nobi Plain, Japan. Paddy Water Environ 4:251–263. doi:10.1007/s10333-006-0056-4

Ishikawa Prefecture (2010) Environmental white book 2009 in Ishikawa Prefecture, Ishikawa. Available via http://www.pref.ishikawa.lg.jp/kankyo/shiryo/hakusyo/documents/h21hakusyo.pdf. Cited 9 March 2014 (in Japanese)

Ishikawa Prefecture (2012) List of amount of intake water by water service facilities. Statistical survey of water service in 2010. Available via http://www.pref.ishikawa.lg.jp/mizukankyo/shiryo/suidou/h22.html. Cited 9 March 2014 (in Japanese)

Iwasaki Y, Ozaki M, Nakamura K et al (2013a) Relationship between increment of groundwater level at the beginning of irrigation period and paddy field area in the Tedori River Alluvial Fan Area, Japan. Paddy Water Environ 11:551–558. doi:10.1007/s10333-012-0348-9

Iwasaki Y, Ozaki M, Nakamura K et al (2013b) Assessment of factors influencing groundwater level changes during irrigation in the Tedori River Fan based on steady state groundwater flow analysis. J Jpn Soc Hydrol Water Res 26(2):99–113 (in Japanese with English abstract)

Japan Meteorological Agency (2008) Global warming projection 7. Available via http://ds.data.jma.go.jp/tcc/tcc/products/gwp/gwp7/index-e.html. Cited 9 March 2014

Kaushal KG, Bhabani SD, Mohamman S et al (2009) Measurement and modeling of soil water regime in a lowland paddy field showing preferential transport. Agr Water Manage 96:1705–1714.

doi:10.1016/j.agwat.2009.06.018

Kayane I. (1980) Groundwater use for snow melting on the road. GeoJournal 4.2:173-181

Khan S, Rana T, Carroll J, et al (2010) Assessment of rice hydraulic loading impacts on groundwater and salinity levels. Paddy Water Environ 8:23–29. doi:10.1007/s10333-009-0171-0

Kotoda K (1989) Estimation of river basin evapotranspiration from consideration of topographies and land use conditions. IAHS Publ 177:271–281

Kukal SS, Aggarwal GC (2002) Percolation losses of water in relation to puddling intensity and depth in a sandy loam rice (*Oryza sativa*) field. Agr Water Manage 57:49–59

Leterme B, Gedeon M, Jacques D Groundwater recharge modeling in the Nete catchment (Belgium) with HYDRUS-1D – MODFLOW package, In: Šimůnek J van Genuchten M TH, Kodešová R (eds) Proc. of the 4th International Conference "HYDRUS Software Applications to Subsurface Flow and Contaminant Transport Problems", March 21-22, 2013, Dept. of Soil Science and Geology, Czech University of Life Sciences, Prague, Czech Republic, ISBN: 978-80-213-2380-3, pp. 235–244, 2013

Liu CW, Chen SK, Jou SW et al (2001) Estimation of the infiltration rate of a paddy field in Yun-Lin Taiwan. Agricultural Systems 68:41–54

Lin L, Zhang ZB, Janssen M et al (2013) Infiltration properties of paddy fields under intermittent irrigation. Paddy Water Environ doi:10.1007/s10333-013-0354-6

Maruyama T, Noto F, Yoshida M et al (2014) Analysis of water balance in the Tedori river alluvial fan areas of Japan: focused on quantitative analysis of groundwater recharge from river and ground surface, especially paddy fields. Paddy Water Environ 12:163–171. doi:10.1007/s10333-013-0373-3

Maruyama T, Noto F, Yoshida M et al (2012) Analysis of water balance at the Tedori River alluvial fan areas in Japan. J Jpn Soc Hydrol Water Res 25(1):20–29 (in Japanese with English abstract)

Matsuno Y, Nakamura K, Masumoto T et al (2006) Prospects for multifunctionality of paddy rice cultivation in Japan and other countries in monsoon Asia. Paddy Water Environ 4:189–197. doi:10.1007/s10333-006-0048-4

Ministry of Land, Infrastructure, Transport and Tourism (2011) National Land Numerical Information Download Service. Available via http://nlftp.mlit.go.jp/ksj/. Cited 9 March 2014

Ministry of Land, Infrastructure, Transport and Tourism (2011) The Nationwide Ocean Wave information network for Ports and HArbourS, (NOWPHAS) Available via http://www.mlit.go.jp/kowan/nowphas/index_eng.html. Cited 9 March 2014

Mitsuno T, Kobayashi S, Maruyama T (1982) Groundwater recharge function of paddy field: a case of

groundwater balance analysis in Nobi Plain. J JSIDRE 50(1):1–18 (in Japanese)

Morita K, Honda T, Nishiura T (2008) For planning of normal discharge of Tedori River. Technical Report of Hokuriku Regional Office of Construction, Ministry of Construction and Transportation. Available via http://www.hrr.mlit.go.jp/library/happyoukai/h20/pdf/c/cj_15kanazawa.pdf. Cited 9 March 2014 (in Japanese)

Mualem Y (1976) A new model for predicting the hydraulic conductivity of unsaturated porous media. Water Resour Res 12:513–522

Murashima K (2009) Investigation and change prediction of irrigation water use. Normal hydrological cycle as a core of irrigation water, Annual Report 2008. Ishikawa Prefectural University, Japan (in Japanese).

Nakumura S, Yudate T, Uchino H et al (2007) Effect of vegetation cover ratio in maize and soybean on weed growth and crop yield: relations to planting density and varieties. Report of the Hokkaido Branch, the Japanese Society of Breeding and Hokkaido Branch, the Crop Science Society of Japan 48:51–52 (in Japanese)

Noto F, Maruyama T, Hayase Y et al (2013a) Evaluation of water resources by snow storage using water balance and tank model method in the Tedori River basin of Japan. Paddy Water Environ 11:113–121. doi:10.1007/s10333-011-0297-8

Noto F, Maruyama T, Hayase Y et al (2013b) Prediction of water resources as snow storage under climate change in the Tedori River basin of Japan. Paddy Water Environ 11:463–471. doi:10.1007/s10333-012-0337-z

Okumaya T (2011) Clarifying hydrogeological structure of Tedori River basin. Research on sound hydrologic cycle as a core of irrigation, Annual Report 2010. Ishikawa Prefectural University, Japan (in Japanese)

Phogat V, Yadav AK, Malik RS et al (2010) Simulation of salt and water movement and estimation of water productivity of rice crop irrigated with saline water. Paddy Water Environ 8:333–346

Raneesh KY, Thampi SG (2013) A simple semi-distributed hydrologic model to estimate groundwater recharge in a humid tropical basin. Water Resour Manage 27:1517–1532. doi:10.1007/s11269-012-0252-5

Satoh T (2002) Studies on techniques for lodging prevention of rice variety “Koshihikari” based on growth diagnosis. Hokuriku Sakumotsu Gakkaiho 37:4–9 (in Japanese)

Shibayama M, Sakamoto T, Takada E et al (2011) Estimating paddy rice leaf area index with fixed point continuous observation of near infrared reflectance using a calibrated digital camera. Plant Prod Sci 14(1):30–46

Shimada S, Hirokawa F, Miyagawa T (1990) Effects of planting data and planting density on a high yielding soybean cultivar grown at drained paddy field in Sanyo District. Jpn J Crop Sci 59(2):257–264 (in Japanese with English abstract)

Šimunek J, Bradford SA (2008) Vadose zone modeling: introduction and importance. Vadose Zone Journal 7(2):581–586

Sugio S, Eto M, Imayama K et al (1999) Fall of unconfined groundwater level caused by change of ground cover condition in Miyazaki city. Journal of Groundwater Hydrology 41(4):253–262 (in Japanese with English abstract)

Takeda G, Udagawa T (1976) Ecological studies on the photosynthesis of winter cereals. III. Changes of the photosynthetic ability of various organs with growth. Jpn J Crop Sci 45(2):357–368 (in Japanese with English abstract)

Toung TP, Wopereis MCS, Marquez JA et al (1994) Mechanisms and control of percolation losses in irrigated puddled rice fields. Soil Sci Soc Am J 58:1794–1803

Tournebize J, Watanabe H, Takagi K et al (2006) The development of a coupled model (PCPF-SWMS) to simulate water flow and pollutant transport in Japanese paddy fields. Paddy Water Environ 4:39–51

Tsuchihara T, Yoshimoto S, Ishida S et al (2010) Environmental Isotope-based Investigation of Hydrological Aspects of Groundwater Recharge and Discharge in Tedori Alluvial Fan. Appl Hydrol 22:11–20 (in Japanese)

Tsujimoto T, Futamata H, Qing X et al (2005) Relation between instream flow and underground water in fluvial fan discussed in river management of the Tedori River. Journal of River Engineering 11:529–534 (in Japanese with English abstract)

Twarakavi NKC, Šimunek J, Seo S (2008) Evaluating interactions between groundwater and vadose zone using the HYDRUS-based flow package for MODFLOW. Vadose Zone J 7:757–768

van Genuchten MTh (1980) A closed-form equation for predicting the hydraulic conductivity of unsaturated soils. Soil Sci Soc Am J 44:892–898

Watanabe S, Yoneda M, Morisawa S et al 2002. Simulation of groundwater level fluctuation and recharge estimation in Kagamihara groundwater basin, Gifu prefecture. Journal of Groundwater Hydrology 44(3):199–211 (in Japanese with English abstract).

Xu X, Huang G, Zhan H et al (2012) Integration of SWAP and MODFLOW-2000 for modeling groundwater dynamics in shallow water table areas. J Hydrol 412-413:70-181. Doi:10.1016/j.kydrol.2011.07.002

Zhu Y, Shi L, Lin L et al (2012) A fully coupled numerical modeling for regional unsaturated-saturated water flow. J Hydrol 475:188–203

Table 1 Hydraulic parameters in HYDRUS-1D

Zone	θ_r	θ_s	α (1/m)	n	K_s (m/d)	l
Plow layer in northern zone	0.0500	0.3710	1.10	1.30	10.0	0.5
Subsoil in northern zone	0.0501	0.3810	2.51	2.50	70.1	0.5
Plow layer in southern zone	0.0587	0.3660	0.964	1.40	6.74	0.5
Subsoil in southern zone	0.0527	0.411	3.36	2.71	100	0.5
Plow layer in coastal zone	0.0501	0.3700	0.998	1.50	9.94	0.5
Subsoil in coastal zone	0.0500	0.3980	3.01	2.72	70.5	0.5

Table 2 Irrigation water management and amount of irrigation water

Term	Irrigation water management	Amount of irrigation water (mm/d)
Late April	Soil puddling	60
Early May to late May	-	20
Early June to mid-June	Mid-summer drainage	Precipitation
Late June to late July	Intermittent irrigation	20
Early August to late August	Intermittent irrigation	5
Early September	Ponding water release	Precipitation

Table 3 Hydraulic conductivities and storage coefficents using MODFLOW

	Zone	Hydraulic conductivity (m/d)	Specific storage (1/m)	Specific yield
Shallow aquifer	Northern zone	8.6×10^{2}	1.0×10^{-4}	0.05
	Southern zone	4.8×10^{1}	1.0×10^{-4}	0.05
	Coastal zone	7.4×10^{2}	6.6×10^{-5}	0.05
	Coastal clay zone	1.1×10^{-3}	1.0×10^{-3}	0.03
Deep aquifer		1.2×10^{0}	1.0×10^{-4}	0.05

Table 4 Change rate of annual groundwater levels

Zone	Change rate of annual groundwater levels (m/y)	
	Hydrological year	Irrigation period
Zone 1	-0.07	-0.08
Zone 2	-0.07	-0.10
Zone 3	-0.03	-0.04
Zone 4	-0.05	-0.08
Zone 5	-0.04	-0.06
Zone 6	-0.02	-0.03

*Positive value indicates groundwater level rise and negative value indicates groundwater level depression.

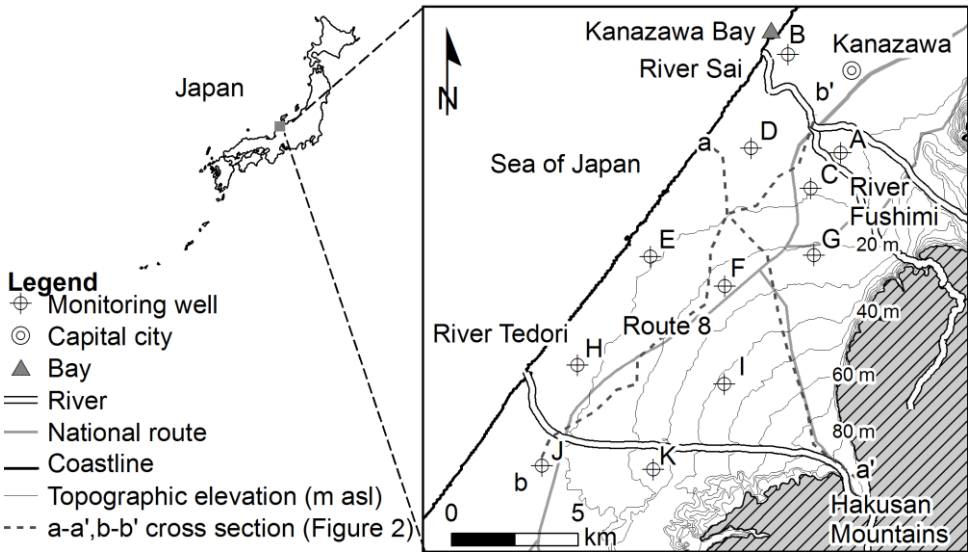

Fig. 1 Outline of the study area

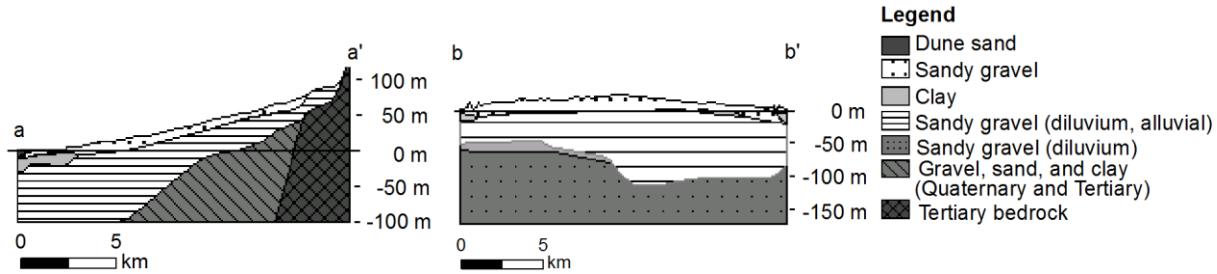

Fig. 2 Hydrogeological conditions across the study area (sections a-a' and b-b' in Fig.1) (Modified From Hokuriku Regional Agricultural Administration Office 1977)

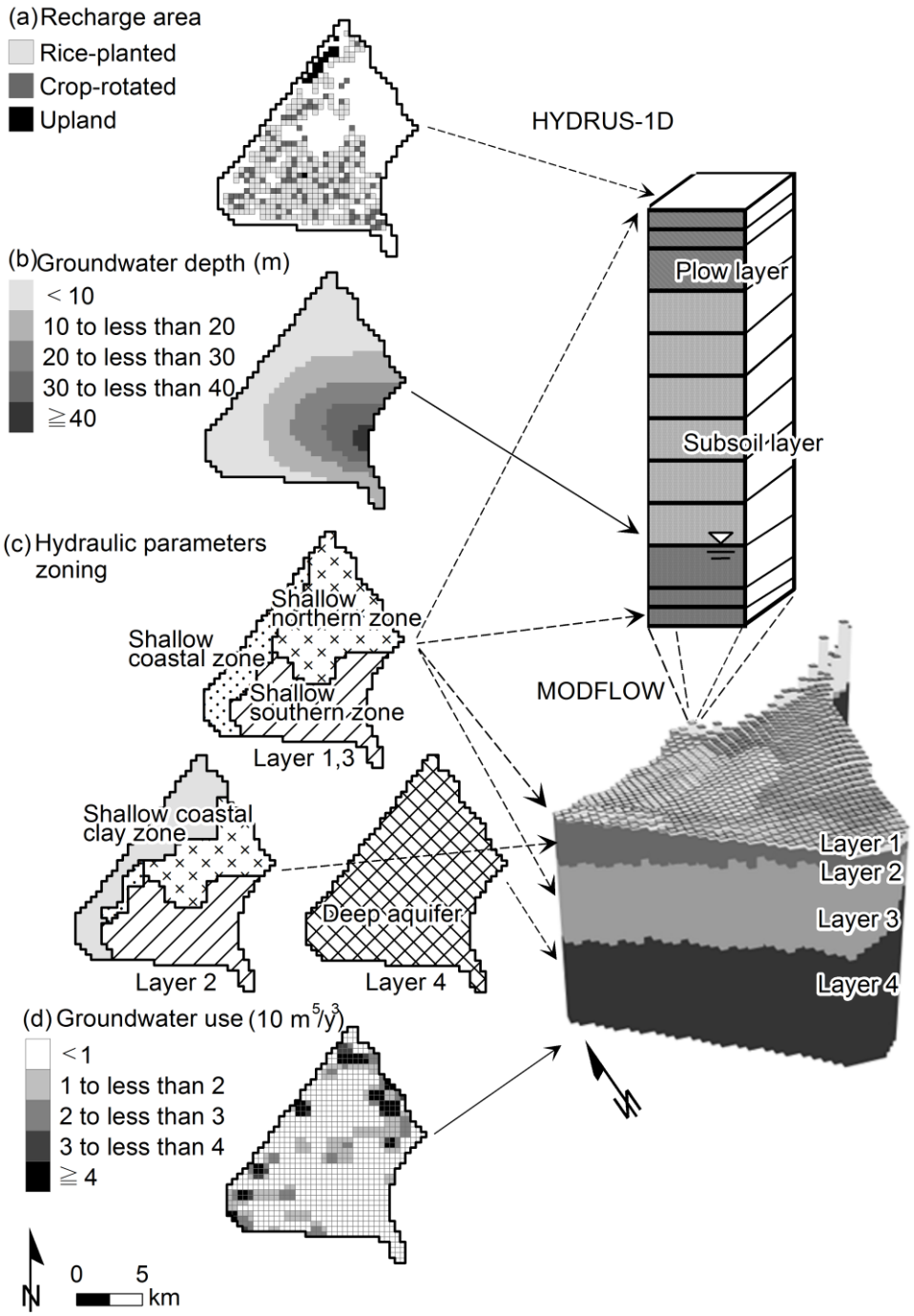

Fig. 3 Input data for HYDRUS-1D and MODFLOW: (a) recharge areas in 2009, (b) groundwater-level depth (non-irrigation period in 1993), (c) hydraulic parameters zoning, (d) annual groundwater use in 1993

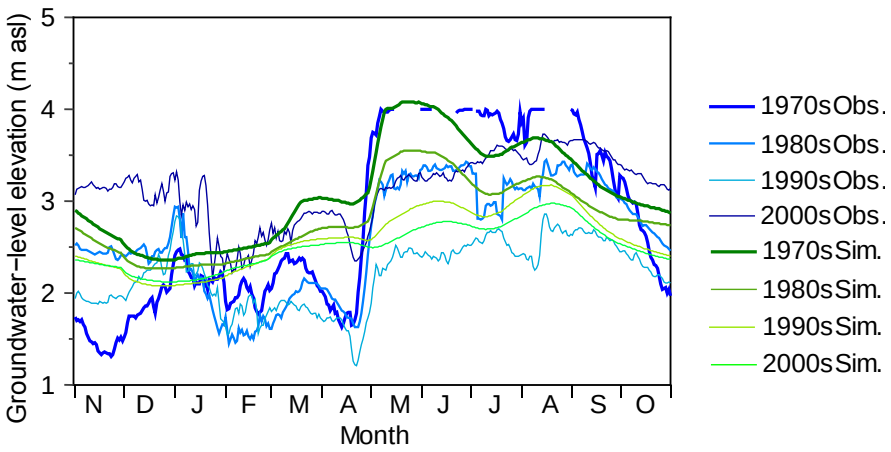

Fig. 4 Calculated and observed groundwater levels averaged by decade in well D

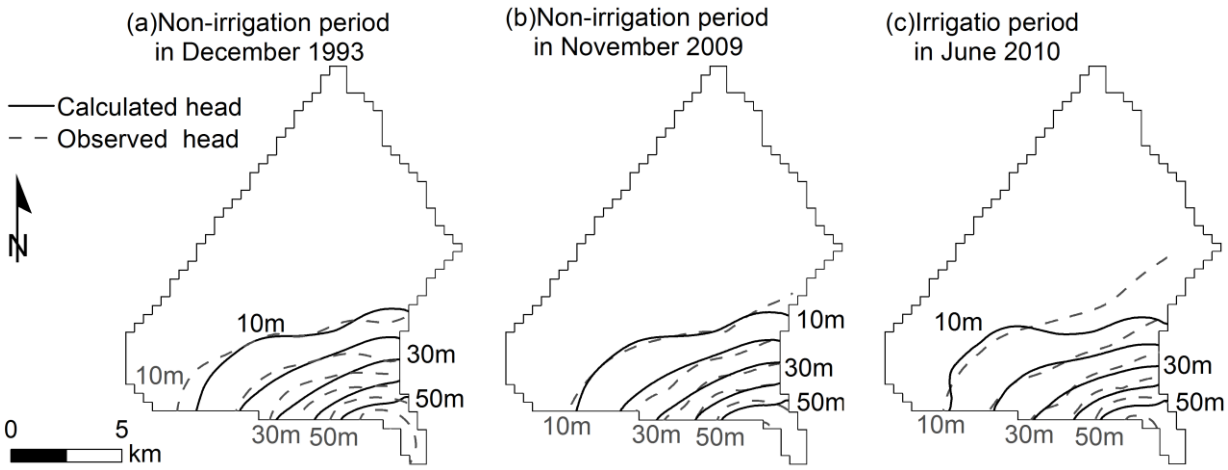

Fig. 5 Calculated and observed groundwater-level elevation contour maps: (a) non-irrigation period in December 1993, (b) non-irrigation period in November 2009, and (c) irrigation period in June 2010

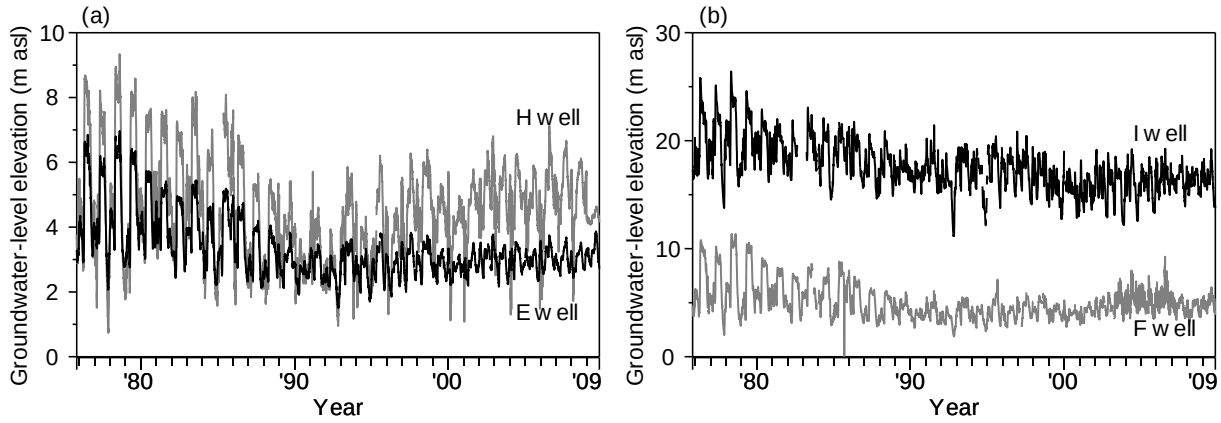

Fig. 6 Temporal changes in observed groundwater-level elevations from 1976 to 2009 at (a) wells E and H, and (b) wells I and F

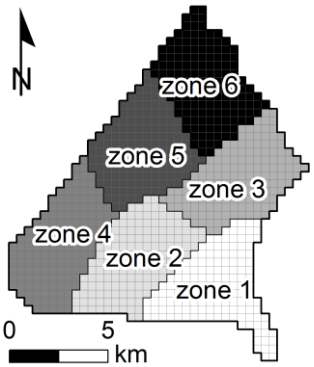

Fig. 7 Partitions of the model domain

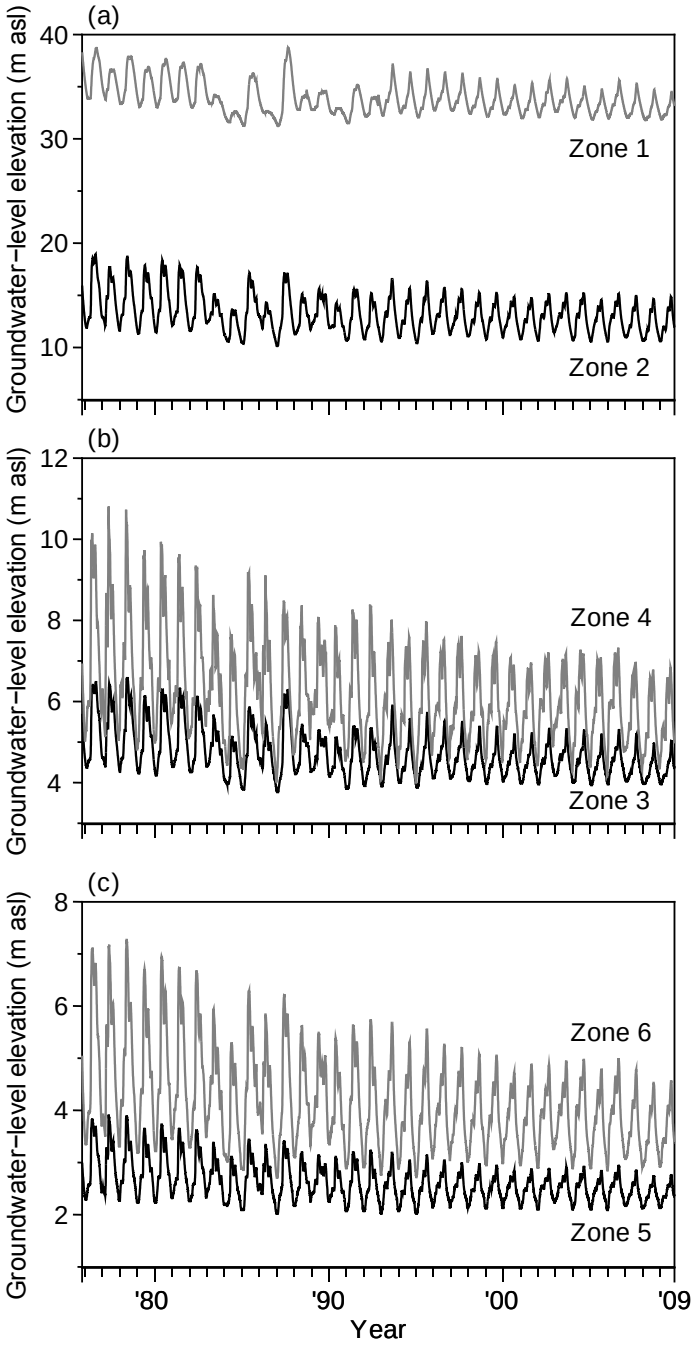

Fig. 8 Temporal changes in calculated groundwater-level elevations averaged in each zone: (a) zones 1 and 2, (b) zones 3 and 4, and (c) zones 5 and 6

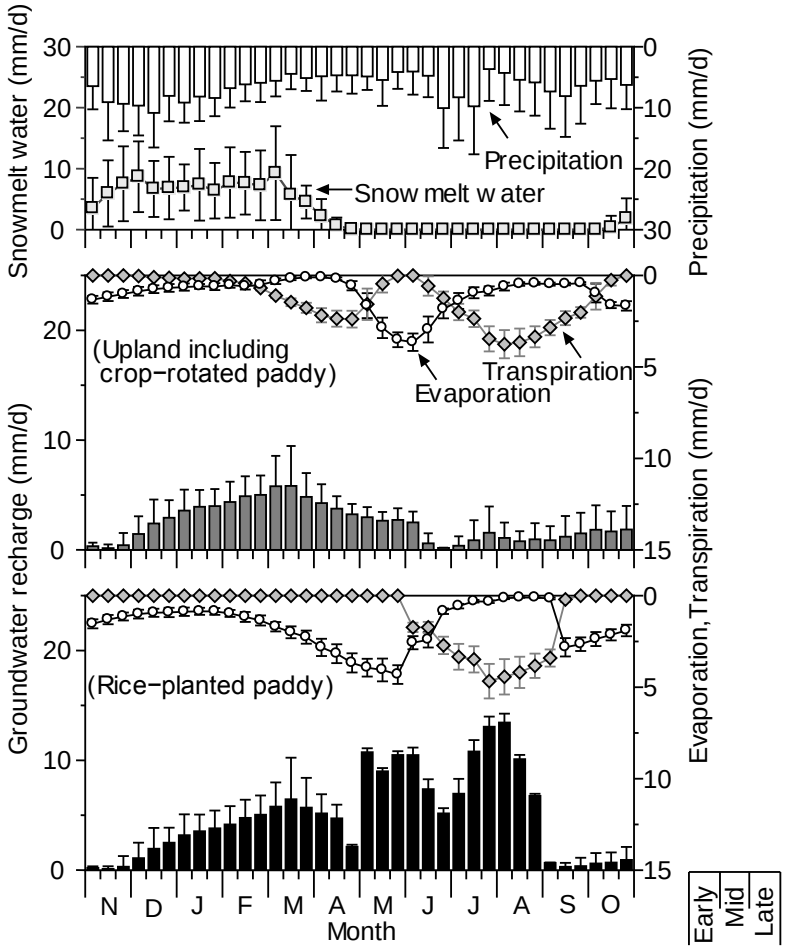

Fig. 9 Seasonal changes in precipitation, snowmelt water, evaporation, transpiration, and groundwater recharge at the unit recharge area. Bars indicate one standard deviation

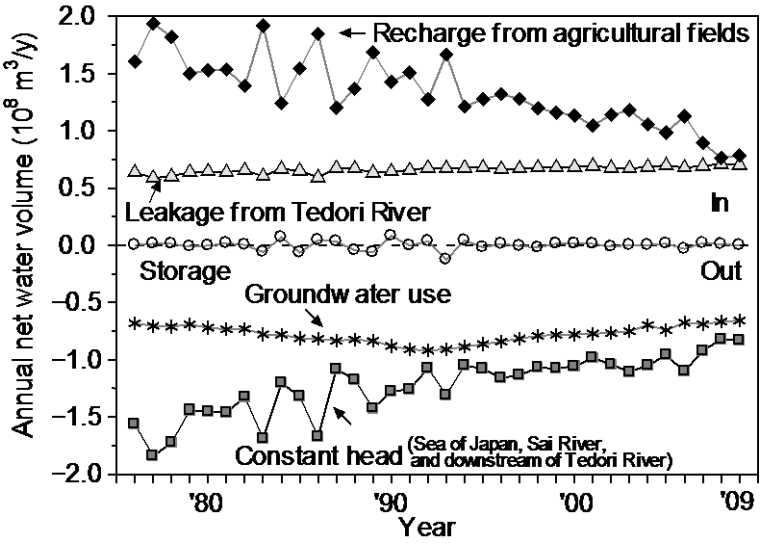

Fig. 10 Annual net water balances for the entire model domain

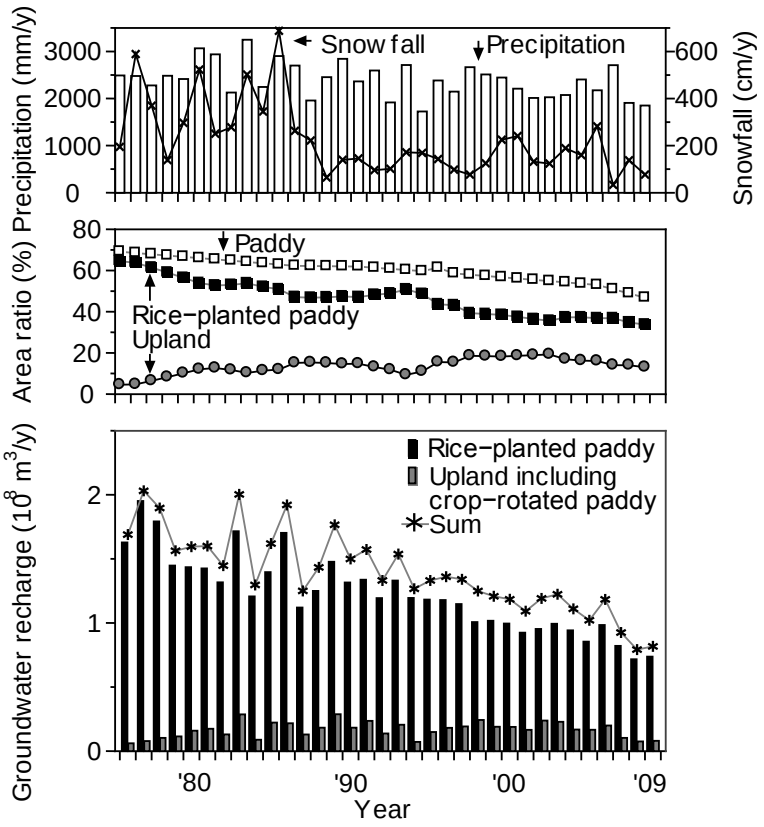

Fig. 11 Annual changes in precipitation, snowfall, area ratio, and groundwater recharge for the entire model domain